Wireless Pers Commun
DOI 10.1007/s11277-008-9546-6

Characterization of Vehicle-to-Vehicle Radio Channels from Measurements at 5.2 GHz

Alexander Paier · Johan Karedal · Nicolai Czink · Charlotte Dumard · Thomas Zemen · Fredrik Tufvesson · Andreas F. Molisch · Christoph F. Mecklenbräuker

Abstract The development of efficient vehicle-to-vehicle (V2V) communications systems requires an understanding of the underlying propagation channels. In this paper, we present results on pathloss, power-delay profiles (PDPs), and delay-Doppler spectra from a high speed measurement campaign on a highway in Lund, Sweden. Measurements were performed at a

This work is an extended version of the conference paper [1].

A. Paier (✉) · C. F. Mecklenbräuker
Institut für Nachrichtentechnik und Hochfrequenztechnik, Technische Universität Wien, Vienna, Austria
e-mail: apaier@nt.tuwien.ac.at

C. F. Mecklenbräuker
e-mail: cfm@nt.tuwien.ac.at

J. Karedal · F. Tufvesson · A. F. Molisch
Department of Electrical and Information Technology, Lund University, Lund, Sweden
e-mail: Johan.Karedal@eit.lth.se

F. Tufvesson
e-mail: Fredrik.Tufvesson@eit.lth.se

A. F. Molisch
e-mail: Andreas.Molish@ieee.org

N. Czink · C. Dumard · T. Zemen
Forschungszentrum Telekommunikation Wien (ftw.), Vienna, Austria
e-mail: czink@ftw.at

C. Dumard
e-mail: dumard@ftw.at

T. Zemen
e-mail: thomas.zemen@ftw.at

N. Czink
Smart Antennas Research Group, Information Systems Lab, Standford University,
Stanford, CA 94305, USA

A. F. Molisch
Mitsubishi Electric Research Labs, Cambridge, USA

carrier frequency of 5.2 GHz with the communicating vehicles traveling on the highway in opposite directions. A pathloss coefficient of 1.8 shows the best fit in the mean square sense with our measurement. The average root mean square (RMS) delay spread is between 263 ns and 376 ns, depending on the noise threshold. We investigate and describe selected paths in the delay-Doppler domain, where we observe Doppler shifts of more than 1,000 Hz.

Keywords Channel measurements · High mobility channel · MIMO measurements · Radio channel characterization · Power-delay profile · Delay-Doppler spectrum

1 Introduction

V2V communications systems have recently drawn great attention, because they have the potential to reduce traffic jams and accident rates. The simulation and performance evaluation of existing systems like IEEE 802.11p [2], as well as the design of future, improved systems, requires a deep understanding of the underlying propagation channels. However, the time-frequency selective fading nature of such V2V channels is significantly different from the well-explored cellular (base-station to mobile) channel, and thus requires distinct measurement campaigns and models. In contrast to cellular systems there exist only a few measurements for V2V communications systems.

Earlier measurements report exclusively on the V2V case with vehicles driving in the *same* direction [3–8], where in [3,4] the radio channel is investigated at 2.4 GHz and in [5–8] in the 5 GHz band. Channel measurements where the vehicles are traveling in the same *and* in opposite directions at a carrier frequency of 3.5 GHz are presented in [9]. Reference [10] reports on V2V measurements in the 900 MHz band between parked vehicles and in [11] the fading statistics of the received signal strength indicator (RSSI) are investigated.

In order to alleviate the current lack of measurements, we recently carried out an extensive measurement campaign in the 5 GHz band in Lund, Sweden. One of the great advantages of these measurements is the high Doppler sampling and the high measurement bandwidth of 240 MHz. This campaign encompassed measurements of vehicle-to-infrastructure (V2I) and V2V scenarios on highways, rural, and urban streets. The current paper concentrates on the evaluation of pathloss, PDP, and delay-Doppler spectrum in a particularly interesting highway V2V measurement run, where the vehicles were traveling in opposite directions. A detailed description of the measurement setup as well as measurement results for V2I and V2V radio channels in other environments can be found in [1,12,13]. In [14] a novel geometry-based stochastic multiple-input multiple-output (MIMO) channel model is presented.

This paper is an extended and enhanced version of [1] and is organized as follows: Section 2 describes the measurement equipment and measurement scenario. Section 3 provides results, including pathloss, PDP, and delay-Doppler spectrum. Section 4 summarizes the paper and presents conclusions.

2 Measurements

2.1 Measurement Equipment

As measurement vehicles, we used two VW LT35 transporters (similar to pickup trucks), which are depicted in Fig. 1a. The measurements that were carried out were MIMO measurements with four antennas at the transmit and receive side, respectively. The MIMO setup impacted the resolvable Doppler frequency because the employed channel sounder,

Fig. 1 (**a**) Photo of the highway from the passenger compartment, (**b**) satellite photo of the highway E22 in the east of Lund (source [16])

Table 1 Measurement parameters

Center frequency, f	5.2 GHz
Measurement bandwidth, BW	240 MHz
Delay resolution, $\Delta\tau = 1/BW$	4.17 ns
Transmit power, P_{Tx}	27 dBm
Test signal length, $\tau_{\max}$	3.2 μs
Number of Tx antenna elements, N_{Tx}	4
Number of Rx antenna elements, N_{Rx}	4
Snapshot time, t_{snap}	102.4 μs
Snapshot repetition rate, t_{rep}	307.2 μs
Number of snapshots, N	32,500
Recording time, t_{rec}	10 s
File size, FS	1 GB
Tx antenna height, h_{Tx}	2.4 m
Rx antenna height, h_{Rx}	2.4 m

RUSK-LUND, is based on the "switched-array" principle [15]. The measurement setup of the RUSK-LUND channel sounder is summarized in Table 1. The snapshot repetition rate was $t_{\mathrm{rep}} = 307.2\ \mu$s, leading to a maximum resolvable Doppler shift of 1.6 kHz corresponding to a maximum speed of 338 km/h. From the channel transfer functions acquired by the channel sounder, we obtain the complex channel impulse responses (IRs) by an inverse Fourier transform using the Hanning window, giving $h(nt_{\mathrm{rep}}, k\Delta\tau, p)$, where $\Delta\tau$ denotes the delay resolution and p denotes the number of the antenna-to-antenna channels out of the 4×4 MIMO configuration. A more detailed description of the measurement equipment and practice can be found in [12].

2.2 Measurement Scenario

In this paper, we present detailed evaluation results from one especially selected measurement run. It is a highway scenario with medium traffic (approximately 1 vehicle per second), where the vehicles traveled in opposite directions. Figure 1a shows the receiver (Rx) vehicle traveling on the opposite lane just before the vehicles were passing. The satellite photo of the highway scenario indicates that the transmitter (Tx) vehicle was heading in southwest direction while the Rx vehicle headed northeast. The Tx and Rx of the channel sounder were equipped with Global Positioning System (GPS) receivers. With these GPS receivers, we recorded the locations and speeds of both measurement vehicles. The speeds agree well with

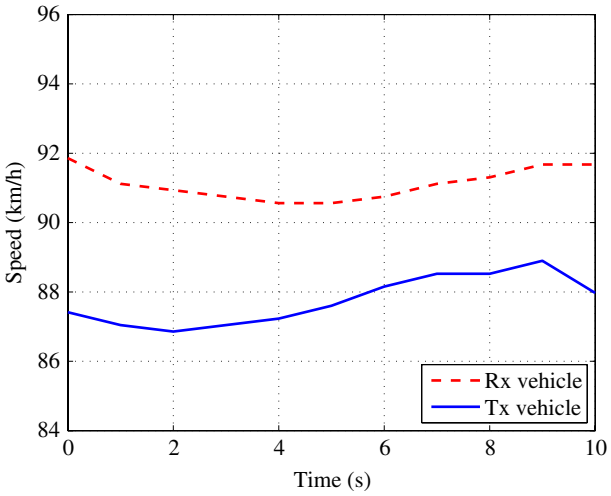

Fig. 2 Speed over time of the two measurement vehicles

those observed on the speedometers (90 km/h) of the vehicles during the measurement run (see Fig. 2). The relative speed between the two vehicles, which is in this case the sum of the speeds of the individual vehicles, is approximately 180 km/h.

3 Evaluation Results

3.1 Pathloss

For calculating the pathloss, the received power was calculated by averaging the magnitude squared of the channel coefficients over 20 wavelengths, in order to average over the small scale fading, and taking the sum over all $K = 769$ delay bins and all $P = 16$ antenna-to-antenna channels, i.e.,

$$P_{\mathrm{Rx}}(i t_{\mathrm{av}}) = \frac{1}{L} \sum_{n=iL}^{(i+1)L-1} \sum_{k=0}^{K-1} \sum_{p=1}^{P} |h(n t_{\mathrm{rep}}, k\Delta\tau, p)|^2. \tag{1}$$

Twenty wavelengths are equal to 1.2 m and thus yield at a relative speed of 180 km/h an averaging time interval of $t_{\mathrm{av}} = 23$ ms, i.e., $L = 75$ snapshots. By investigations of the stationarity time in [13], it was found that in this particular scenario, the channel can be considered stationary during a time interval of 23 ms. After calculating the received power and investigating the noise level, we used a noise threshold of -102.7 dBm. In the following, we show that a noise threshold does not have a large effect on the calculation of the pathloss, but does affect the calculation of the mean excess delay and RMS delay spread (see Sect. 3.2). All values below the noise threshold are considered as noise and therefore set to zero. The pathloss was calculated by taking the difference of the transmitted power of 27 dBm and the received power in logarithmic scale

$$PL|_{\mathrm{dB}} = P_{\mathrm{Tx}}|_{\mathrm{dBm}} - P_{\mathrm{Rx}}|_{\mathrm{dBm}}. \tag{2}$$

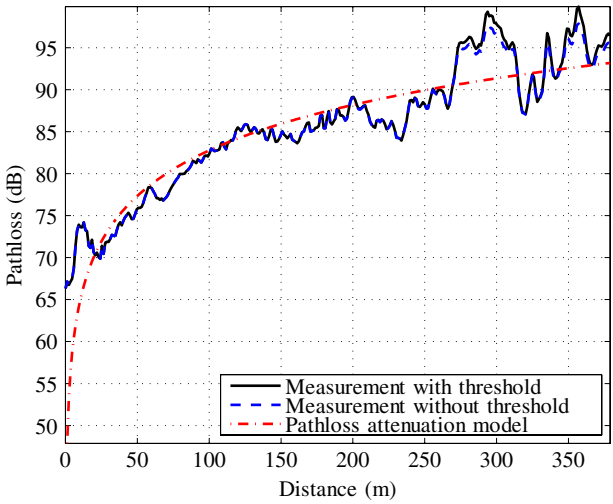

Fig. 3 Comparison between measured pathloss (with and without noise threshold) and a pathloss model with attenuation coefficient 1.8

Figure 3 presents the pathloss PL (with and without noise threshold). We fitted the measured pathloss to the standard model [17, Chap. 4]

$$PL_{\text{model}}|_{\text{dB}} = -20 \cdot \log_{10}\left(\frac{c_0}{4\pi f}\right) + n_{\text{att}} \cdot 10 \cdot \log_{10}(d), \tag{3}$$

where c_0 is the speed of light, f is the carrier frequency, d is the distance between Tx and Rx, and n_{att} is the attenuation coefficient. An attenuation coefficient of 1.8 yields the lowest RMS error of 3.3 dB considering the noise threshold and 3.1 dB without considering the noise threshold. The measurement results are taken from the first 7.5 s of our measurement run, where the two vehicles were approaching each other. In Fig. 3, we observe that the pathloss curves calculated with and without considering the noise threshold are strongly overlapping. In our measurement small differences only occur at distances greater than 250 m (see Fig. 3). This is because large pathlosses mean small Rx power and in this case the noise power affects the result. We conclude that the inclusion of a noise threshold has no significant impact on the pathloss.

3.2 Power-Delay Profile

Similar to the calculation of the received power, we calculated the short-time average PDP by averaging the magnitude squared IRs over 20 wavelengths, $L = 75$ snapshots, and taking the sum over all $P = 16$ antenna-to-antenna channels

$$P_{\text{PDP}}(it_{\text{av}}, k\Delta\tau) = \frac{1}{L}\sum_{n=iL}^{(i+1)L-1}\sum_{p=1}^{P}|h(nt_{\text{rep}}, k\Delta\tau, p)|^2. \tag{4}$$

Using this calculation, we obtained 433 averaged PDPs ($i = 1, \ldots, 433$) for the 10 s measurement run. Figure 4a shows the strong LOS path with delay decreasing until 7.5 s (vehicles passing) and increasing delay afterwards. There are also several paths that are approximately parallel to the LOS path. These paths result from reflections from vehicles that are traveling

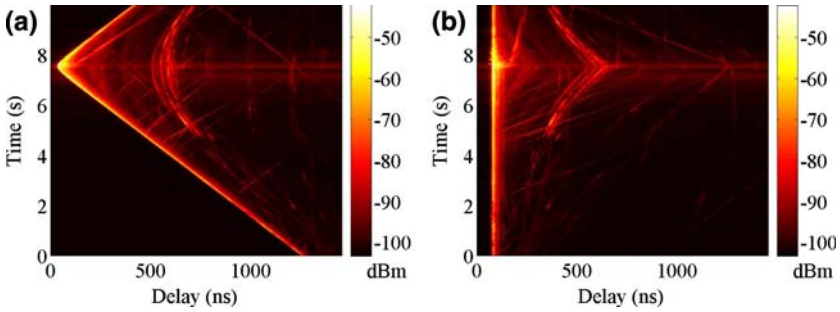

Fig. 4 (**a**) Average PDP, (**b**) average PDP with shifted LOS paths to delay 83 ns

with approximately the same speed as our measurement vehicles. Such a path is exactly parallel to the LOS path if the speed of the reflecting vehicle and the measurement vehicle are equal. Further, there is a group of paths from approximately 5–10 s, whose delays are slightly decreasing from a delay of about 700 ns to 600 ns until a time of 7.5 s and increasing afterwards. These paths are much stronger than most of the paths, reflected from vehicles. The most likely explanation for this group of paths is scattering at factory buildings in the southeast of the highway, see Fig. 1b. Note that such paths should show a Doppler shift that is less than the Doppler shift of the LOS path, because the angle between driving direction and wave propagation direction is larger than zero. We will show this in Sect. 3.3.

In Fig. 4b, the maximum of the LOS path is shifted to a constant delay of 83 ns. These shifted paths are used for all further calculations of the PDPs and delay-Doppler spectra in this paper, except for the calculation of the mean excess delay, because there we need a shift to the constant delay of zero. The delay of 83 ns is chosen arbitrarily in order to see also the increasing part of the LOS path before its maximum.

In the following, we calculate the mean excess delay and RMS delay spread with and without considering a noise threshold, in order to show the impact of such a threshold. The mean excess delay of discrete PDPs can be computed as [17, Chap. 6.5]

$$\bar{\tau}(it_{\mathrm{av}}) = \sum_{k=0}^{K-1} k\Delta\tau\, P_{\mathrm{PDP}}(it_{\mathrm{av}}, k\Delta\tau) \Big/ P_{\mathrm{Rx}}(it_{\mathrm{av}}). \tag{5}$$

The RMS delay spread is the square root of the second central moment of the PDP [17, Chap. 6.5]

$$\tau_{\mathrm{rms}}(it_{\mathrm{av}}) = \sqrt{\sum_{k=0}^{K-1} (k\Delta\tau - \bar{\tau}(it_{\mathrm{av}}))^2 P_{\mathrm{PDP}}(it_{\mathrm{av}}, k\Delta\tau) \Big/ P_{\mathrm{Rx}}(it_{\mathrm{av}})}. \tag{6}$$

Figure 5 shows the RMS delay spread over time with and without a noise threshold. Similar to the comparison of pathlosses in Fig. 3, we observe differences only at small received powers at $t < 4$ s. The differences are so large that they influence also the mean RMS spread over 10 s. In the vicinity, where the vehicles are passing, the received power is higher, and therefore the threshold does not affect the RMS delay spread results. In order to get one average mean

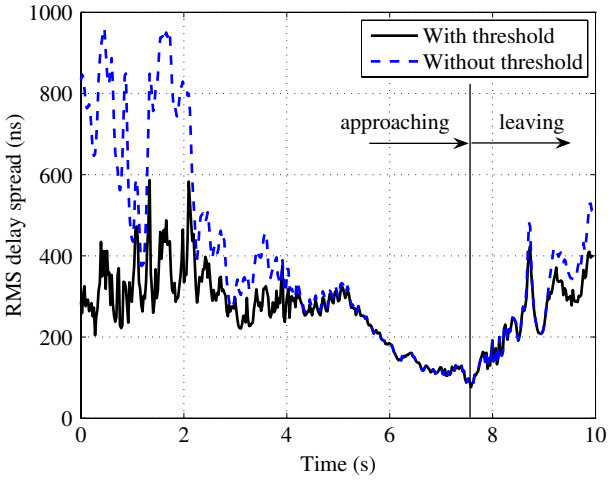

Fig. 5 RMS delay spread with and without noise threshold

Table 2 Average mean excess delay and average RMS delay spread with and without noise threshold

	Av. mean excess delay $\bar{\tau}_{\text{av}}$	Av. RMS delay spread $\tau_{\text{rms,av}}$
With noise threshold	58 ns	263 ns
Without noise threshold	129 ns	376 ns

excess delay, $\bar{\tau}_{\text{av}}$, and one average RMS delay spread, $\tau_{\text{rms,av}}$, for the 10 s measurement run, we average over all 433 values

$$\bar{\tau}_{\text{av}} = \frac{1}{433} \sum_{i=1}^{433} \bar{\tau}(i t_{\text{av}}), \tag{7}$$

$$\tau_{\text{rms,av}} = \frac{1}{433} \sum_{i=1}^{433} \tau_{\text{rms}}(i t_{\text{av}}). \tag{8}$$

Table 2 summarizes these results calculated with and without a noise threshold. Considering a noise threshold implies a much higher impact on these calculations than on the calculations of the pathloss in the previous section. This is because for the calculation of the mean excess delay and RMS delay spread, the discrete PDPs at each delay bin are weighted with the delay $k\Delta\tau$. Therefore the noise, which occurs at larger delays has more impact because of the larger weighting factors. This is not the case for the pathloss calculation, where we just sum up over all PDPs. These results show us that it is important to set a well-selected noise threshold for the calculation of the mean excess delay and the RMS delay spread. The influence of different noise thresholds on the RMS delay spread is described in more detail in [18].

Six short-time PDPs, each over a duration of 23 ms, from 5 s to 5.5 s are depicted in Fig. 6. There are some changes of the short-time PDP over this time period. At a delay of 83 ns, the LOS path is constant over the 0.5 s period, which is a consequence of shifting this path to this delay. Shortly after the LOS path, we observe a small peak with increasing delay. The second

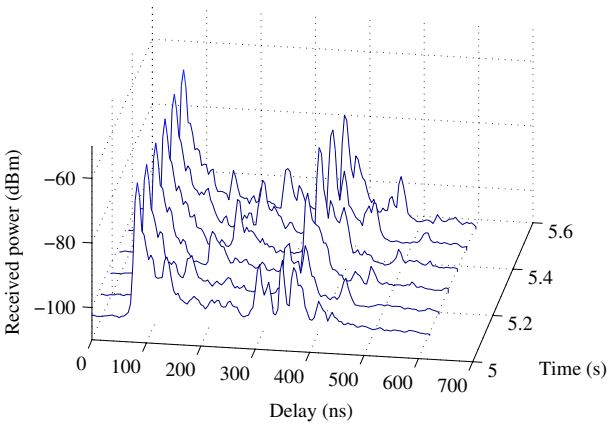

Fig. 6 Short-time average PDPs from 5 s to 5.5 s

strongest peak in this figure, at a delay of approximately 370 ns, comes from scattering at the factory buildings, described above. This path is changing from three smaller peaks in the first PDP to more or less one larger peak in the last PDP. This demonstrates the non-stationarity of the radio channel over the time period of 0.5 s.

3.3 Delay-Doppler Spectrum

In order to validate our measurement, we compared the measured LOS Doppler shift to the theoretical value

$$\nu(t) = -\frac{v}{\lambda}\cos(\gamma(t)). \tag{9}$$

In this equation, $v = 180$ km/h is the relative speed between the two vehicles, $\lambda = 58$ mm is the wavelength, and $\gamma(t)$ is the angle between driving direction and LOS path direction. Figure 7 shows the range between the two vehicles in the upper figure and the calculated and measured Doppler shift in the figure below. The measured Doppler shift (crosses) and the calculated Doppler shift (curve) fit very well.

We estimated the delay-Doppler spectrum

$$P_{\mathrm{DD}}(r\Delta\nu, k\Delta\tau) = \sum_{p=1}^{P} |f_{\mathrm{fft}}(h(nt_{\mathrm{rep}}, k\Delta\tau, p))|^2, \tag{10}$$

using the fast-Fourier transform (FFT) from the time domain indexed by n to the Doppler domain indexed by r. Subsequently we took the sum of the magnitude squared of these terms over all 16 channels. For the short-time delay-Doppler spectrum, we perform the FFT over 75 snapshots, which results in a Doppler resolution of $\Delta\nu = 43$ Hz for $-37 \leq r \leq 37$. Figure 8 shows the short-time delay-Doppler spectrum normalized to its maximum after a time of 5 s of the measurement run. In the following, we describe peaks with their maxima at (i) 83 ns/868 Hz, (ii) 371 ns/543 Hz, and (iii) 304 ns/−1107 Hz. Peak (i) is the LOS path with a Doppler shift of 868 Hz, corresponding to a relative speed of 180 km/h between Tx and Rx, which agrees exactly with the intended speed. Positive Doppler frequencies indicate that the vehicles are approaching. Peak (ii) represents the path scattered at the factory buildings with a Doppler shift of 543 Hz (see Fig. 9). Note that this Doppler shift, lying between zero and

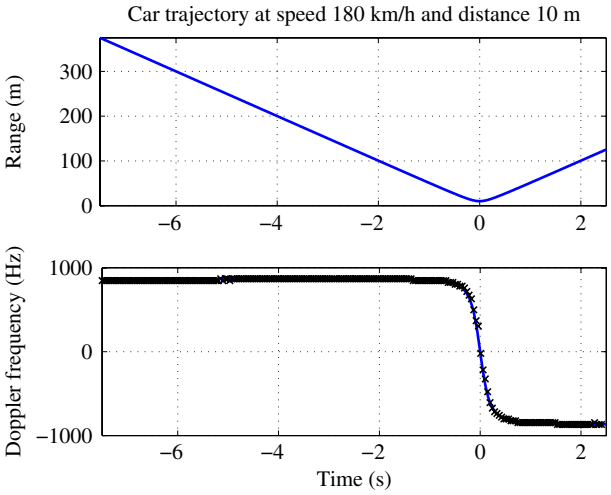

Fig. 7 Comparison of measured and calculated Doppler shifts of the LOS path

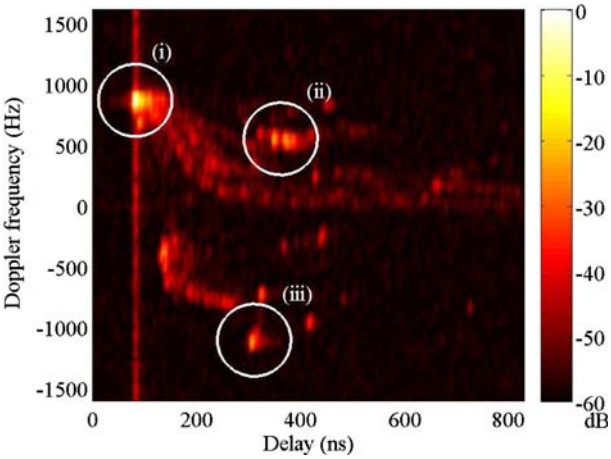

Fig. 8 Short-time delay-Doppler spectrum in logarithmic scale at 5 s

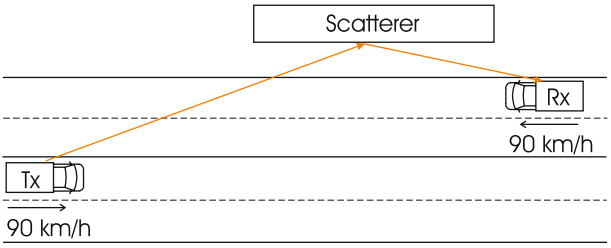

Fig. 9 Doppler shift scenario (ii), leading to a shift of 543 Hz

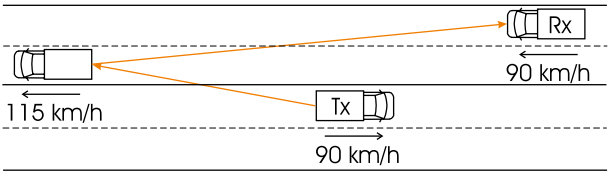

Fig. 10 Doppler shift scenario (iii), leading to a shift of −1107 Hz

the LOS Doppler shift, is congruent with our deductions in Sect. 3.2. Considering the delay of peak (iii), we can find in Fig. 4 that it is approximately parallel to the LOS path delay. With a Doppler shift of −1107 Hz this path is reflected at a vehicle with a speed of 115 km/h which is thus 25 km/h faster than the measurement vehicles. Figure 10 depicts this scenario.

4 Conclusions

In this paper, we presented results from a V2V measurement campaign at 5.2 GHz in a typical highway scenario. The RMS delay spread ranges from 263 ns to 376 ns, and the average mean excess delay is between 58 ns and 129 ns. It is noteworthy that the delay-Doppler spectrum *cannot* be described by the standard model, i.e., a product of exponentially-decaying PDPs and Jakes Doppler spectrum. Rather, we found multiple clusters in the delay domain, each with distinct Doppler spectra. More detailed modeling considerations will be discussed in [14]. Beside a strong LOS path, we observed several paths approximately parallel to the LOS path, which were reflected at other vehicles on the highway. Other strong paths were found, scattering at factory buildings next to the highway. These paths have a Doppler shift less than the Doppler shift of the LOS path, which is in accordance with the theory.

Acknowledgements We would like to thank RIEGL Laser Measurement Systems GmbH and MEDAV GmbH for their generous support. This work was carried out with partial funding from Kplus and WWTF in the ftw. projects I0 and I2 and partially by an INGVAR grant of the Swedish Strategic Research Foundation (SSF), the SSF Center of Excellence for High-Speed Wireless Communications (HSWC), and COST 2100. Finally, we would like to thank Helmut Hofstetter for guidance and help during the measurement campaign.

References

1. Paier, A., Karedal, J., Czink, N., Hofstetter, H., Dumard, C., Zemen, T., Tufvesson, F., Molisch, A. F., & Mecklenbräuker, C. F. (2007). Car-to-car radio channel measurements at 5 GHz: Pathloss, power-delay profile, and delay-Doppler spectrum. In *IEEE International Symposium on Wireless Communication Systems (ISWCS 2007)*, 17–19 October 2007, pp. 224–228.
2. 802.11p. (2006). Draft amendment to wireless LAN medium access control (MAC) and physical layer (PHY) specifications: Wireless access in vehicular environments. IEEE P802.11p/D0.26, January 2006.
3. Acosta, G., Tokuda, K., & Ingram, M. A. (2004). Measured joint Doppler-delay power profiles for vehicle-to-vehicle communications at 2.4 GHz. In *Global Telecommunications Conference 2004*, Vol. 6, 29 November–3 December 2004, pp. 3813–3817.
4. Acosta, G., & Ingram, M. A. (2006). Model development for the wideband expressway vehicle-to-vehicle 2.4 GHz channel. In *IEEE Wireless Communications and Networking Conference (WCNC) 2006*, Vol. 3, 3–6 April 2006, pp. 1283–1288.
5. Acosta-Marum, G., & Ingram, M. A. (2006). Doubly selective vehicle-to-vehicle channel measurements and modeling at 5.9 GHz. In *Wireless Personal Multimedia Communications (WPMC) 2006*, 17–20 September 2006.

6. Maurer, J., Fügen, T., & Wiesbeck, W. (2002). Narrow-band measurement and analysis of the inter-vehicle transmission channel at 5.2 GHz. In *Vehicular Technology Conference (VTC) 2002*, Vol. 3, 6–9 May 2002, pp. 1274–1278.
7. Matolak, D. W., Sen, I., Xiong, W., & Yaskoff, N. T. (2005). 5 GHz wireless channel characterization for vehicle to vehicle communications. In *IEEE Military Communications Conference (MILCOM 2005)*, Vol. 5, 17–20 October 2005, pp. 3016–3022.
8. Cheng, L., Henty, B. E., Stancil, D. D., Bai, F., & Mudalige, P. (2007). Mobile vehicle-to-vehicle narrow-band channel measurement and characterization of the 5.9 GHz dedicated short range communication (DSRC) frequency band. *IEEE Journal on Selected Areas in Communications, 25*(8), 1501–1516.
9. Eggers, P. C. F., Brown, T. W. C., Olesen, K., & Pedersen, G. F. (2007). Assessment of capacity support and scattering in experimental high speed vehicle to vehicle MIMO links. In *65th IEEE Vehicular Technology Conference (VTC2007-Spring)*, 22–25 April 2007, pp. 466–470.
10. Davis, J. S., & Linnartz, J. P. M. G. (1994). Vehicle to vehicle RF propagation measurements. In *Conference Record of the Twenty-Eighth Asilomar Conference on Signals, Systems and Computers, 1994*, Vol. 1, 31 October–2 November 1994, pp. 470–474.
11. Yin, J., Holland, G., ElBatt, T., Bai, F., & Krishnan, H. (2006). DSRC channel fading analysis from empirical measurement. In *First International Conference on Communications and Networking in China (ChinaCom '06)*, 25–27 October 2006, pp. 1–5.
12. Paier, A., Karedal, J., Czink, N., Hofstetter, H., Dumard, C., Zemen, T., Tufvesson, F., Mecklenbräuker, C. F., & Molisch, A. F. (2007). First results from car-to-car and car-to-infrastructure radio channel measurements at 5.2 GHz. In *International Symposium on Personal, Indoor and Mobile Radio Communications (PIMRC 2007)*, 3–7 September 2007, pp. 1–5.
13. Paier, A., Zemen, T., Bernadó, L., Matz, G., Karedal, J., Czink, N., Dumard, C., Tufvesson, F., Molisch, A. F., & Mecklenbräuker, C. F. (2008). Non-WSSUS vehicular channel characterization in highway and urban scenarios at 5.2 GHz using the local scattering function. In *International Workshop on Smart Antennas (WSA 2008)*, 26–27 February 2008, pp. 9–15.
14. Karedal, J., Tufvesson, F., Czink, N., Paier, A., Dumard, C., Zemen, T., Mecklenbräuker, C. F., & Molisch, A. F. (2008). A geometry-based stochastic MIMO model for vehicle-to-vehicle communications. *IEEE Transactions on Wireless Communications*, 2008, to be submitted.
15. Thomä, R., Hampicke, D., Richter, A., Sommerkorn, G., Schneider, A., Trautwein, U., & Wirnitzer, W. (2000). Identification of time-variant directional mobile radio channels. *IEEE Transactions on Instrumentation and Measurement, 49*, 357–364.
16. http://hitta.se, January, 2008.
17. Molisch, A. F. (2005). *Wireless Communications*. IEEE-Press, Wiley.
18. Rossi, J.-P. (1999). Influence of measurement conditions on the evaluation of some radio channel parameters. *IEEE Transactions on Vehicular Technology, 48*, 1304–1316.

Author Biographies

Alexander Paier was born in Bruck/Mur, Austria. From 1999 to 2006 he studied electrical engineering with special subject communications and information technology at the Vienna University of Technology, where he received his Dipl.-Ing. (MSc) degree in 2006. Since July 2006 he is working as research assistant on his doctoral thesis at the Institute of Communications and Radio-Frequency Engineering also at the Vienna University of Technology. He participates in the COST Action 2100 "Pervasive Mobile and Ambient Wireless Communications". His current research interests focus on channel sounding and modeling for vehicular communication networks.

Johan Karedal received the M.S. degree in engineering physics in 2002 from Lund University in Sweden. In 2003, he started working towards the Ph.D. degree at the Department of Electroscience, Lund University, where his research interests are on channel measurement and modeling for MIMO and UWB systems. Johan has participated in the European research initiative "MAGNET".

Nicolai Czink was born in Vienna, Austria, in 1979. He received the Dipl.-Ing. (MSc) degree in 2004 and Dr.techn. (PhD) degree in 2008, both with distinction from Technische Universität Wien, Vienna, Austria. In 2008, he received an Erwin Schrödinger Fellowship award from the Austrian Science Fund (FWF) to join Stanford University as postdoctoral scholar. He is also Senior Researcher at the Forschungszentrum Telekommunikation Wien (ftw.) in the area of wireless communications. His main research focus is radio channel modeling and parameter estimation, as well as cooperative wireless communications.

Charlotte Dumard was born in Paris, France. She received a double Master of Science Degree from the Royal Institue of Technology (KTH) in Stockholm, Sweden and the École Supérieure d'Électricité (Supélec) in Gif-sur-Yvette, France, both 2002. Since September 2004 Charlotte Dumard is with the Telecommunications Research Center Vienna (ftw.), working as a Junior Researcher in the projects "Future Mobile Communications Systems—Mathematical Modeling, Analysis, and Algorithms for Multi Antenna Systems" and later on "Cooperative Communications in Traffic Telematics", both funded by the Vienna Science and Technology Fund (Wiener Wissenschafts-, Forschungs- und Technologiefonds, WWTF). Since February 2006 she is a Ph.D. Student at the Vienna University of Technology. Her research interest are low-complexity transceiver design for time-varying MIMO channels as well as distributed signal processing.

Thomas Zemen (S'03–M'05) was born in Mödling, Austria. He received the Dipl.-Ing. degree (with distinction) in electrical engineering from Vienna University of Technology in 1998 and the doctoral degree (with distinction) in 2004. He joined Siemens Austria in 1998 where he worked as hardware engineer and project manager for the radio communication devices department. He engaged in the development of a vehicular GSM telephone system for a German car manufacturer. Since October 2003 Thomas Zemen has been with the Telecommunications Research Center Vienna. His research interests include orthogonal frequency division multiplexing (OFDM), multi-user detection, time-variant channel estimation, iterative MIMO receiver structures, cooperative communication systems, software defined radio concepts, vehicle-to-vehicle channel measurements and modeling. Since 2008 Thomas Zemen works as key researcher in the area of mobile communications and coordinates the research activities in the sector intelligent transportation. He leads the project "Cooperative Communications for Traffic Telematics" which is funded by the Vienna Science and Technology Fund (Wiener Wissenschafts-, Forschungs- und Technologiefonds, WWTF). He is the speaker of the national research network for "Signal and Information Processing in Science and Engineering" funded by the Austrian Science Fund (FWF). Dr. Zemen teaches "MIMO Communications" as external lecturer at Vienna University of Technology.

Fredrik Tufvesson was born in Lund, Sweden in 1970. He received the M.S. degree in Electrical Engineering in 1994, the Licentiate Degree in 1998 and his Ph.D. in 2000, all from Lund University in Sweden. After two years at a startup company developing mesh network technologies, Fredrik is now associate professor in Radio systems at the department of Electrical and Information Technology, Lund University. His main research interests are channel measurements and modeling for wireless communication, including channels for both MIMO and UWB systems. Beside this, he also works with channel estimation and synchronization problems, OFDM system design and UWB transceiver design.

Andreas F. Molisch received the Dipl.-Ing., Dr. techn., and habilitation degrees from the Technical University Vienna (Austria) in 1990, 1994, and 1999, respectively. From 1991 to 2000, he was with the TU Vienna, becoming an associate professor there in 1999. From 2000 to 2002, he was with the Wireless Systems Research Department at AT&T (Bell) Laboratories Research in Middletown, NJ. Since then, he has been with Mitsubishi Electric Research Labs, Cambridge, MA, where he is now a Distinguished Member of Technical Staff and Chief Wireless Standards Architect. He is also professor and chairholder for radio systems at Lund University, Sweden. Dr. Molisch has done research in the areas of SAW filters, radiative transfer in atomic vapors, atomic line filters, smart antennas, and wideband systems. His current research interests are measurement and modeling of mobile radio channels, UWB, cooperative communications, and MIMO systems. Dr. Molisch has authored, co-authored or edited four books (among them the recent textbook Wireless Communications, Wiley-IEEE Press), eleven book chapters, some 100 journal papers, and numerous conference contributions. Dr. Molisch is an editor of the IEEE Trans. Wireless Comm., co-editor of recent or upcoming special issues in J. Wireless Comm. Mob. Comp., IEEE-JSAC, and the Proceedings of the IEEE. He has been member of numerous TPCs, vice chair of the TPC of VTC 2005 spring, general chair of ICUWB 2006, TPC co-chair of the wireless symposium of Globecomm 2007, and TPC chair of Chinacom2007. He

has participated in the European research initiatives “COST 231”, “COST 259”, and “COST 273”, where he was chairman of the MIMO channel working group, he was chairman of the IEEE 802.15.4a channel model standardization group, and is also chairman of Commission C (signals and systems) of URSI (International Union of Radio Scientists). Dr. Molisch is a Fellow of the IEEE, a Fellow of the IET, an IEEE Distinguished Lecturer, and recipient of several awards.

Christoph F. Mecklenbräuker received the Dipl.-Ing. degree in Electrical Engineering from Vienna University of Technology in 1992 and the Dr.-Ing. degree from Ruhr-University of Bochum in 1998, respectively. His doctoral thesis was awarded with the Gert Massenberg Prize 1998. During 1997–2000, he worked for the Mobile Networks Radio department of Siemens AG Austria where he participated in the European Project “Future Radio Wideband Multiple Access Systems (FRAMES)”. He was a delegate to the Third Generation Partnership Project (3GPP) and engaged in the standardisation of the radio access network for UMTS. From June 2000 on, he was a senior researcher at the Telecommunications Research Center Vienna (ftw.) in the field of mobile communications, key researcher since November 2002, and proxy since July 2003. Since beginning 2006, he coordinates the project “Multiple-Access Space-Time Coding Testbed” (MASCOT) within the Sixth Framework Programme (FP6) of the European Union. He participates in the COST Action 2100 “Pervasive Mobile and Ambient Wireless Communications”. In October 2006, he joined the Institute of Communications and Radio Frequency Engineering at Vienna University of Technology as a full professor. His current research interests include vehicular networks, ultra-wideband radio (UWB), and MIMO-OFDM based transceiver algorithms.